Optimal storage and retrieval of single-photon waveforms

Shuyu Zhou,[1] Shanchao Zhang,[1] Chang Liu,[1] J. F. Chen,[1] Jianming Wen,[2] M. M. T. Loy,[1] G. K. L. Wong,[1] and Shengwang Du[1,*]

[1]*Department of Physics, The Hong Kong University of Science and Technology, Clear Water Bay, Kowloon, Hong Kong, China*
[2]*Institute for Quantum Information Science and Department of Physics and Astronomy, University of Calgary, Calgary T2N 1N4, Alberta, Canada*
[*]*dusw@ust.hk*

http://physics.ust.hk/dusw/

Abstract: We report an experimental demonstration of optimal storage and retrieval of heralded single-photon wave packets using electromagnetically induced transparency (EIT) in cold atoms at a high optical depth. We obtain an optimal storage efficiency of (49±3)% for single-photon waveforms with a temporal likeness of 96%. Our result brings the EIT quantum light-matter interface closer to practical quantum information applications.

OCIS codes: (270.0270) Quantum optics; (270.5585) Quantum information and processing.

References and links

1. A. I. Lvovsky, B. C. Sanders, and W. Tittel, "Optical quantum memory," Nat. Photonics **3**, 706–714 (2009).
2. C. Simon, H. de Riedmatten, M. Afzelius, N. Sangouard, H. Zbinden, and N. Gisin, "Quantum repeaters with photon pair sources and multimode memories," Phys. Rev. Lett. **98**, 190503 (2007).
3. L.-M. Duan, M. D. Lukin, J. I. Cirac, and P. Zoller, "Long-distance quantum communication with atomic ensembles and linear optics," Nature **414**, 413–418 (2001).
4. S. E. Harris, "Electromagnetically induced transparency," Phys. Today **50**, 36–42 (1997).
5. M. Fleischhauer, A. Imamoglu, and J. P. Marangos, "Electromagnetically induced transparency: Optics in coherent media," Rev. Mod. Phys. **77,** 633–673 (2005).
6. C. Liu, Z. Dutton, C. H. Behroozi, and L. V. Hau, "Observation of coherent optical information storage in an atomic medium using halted light pulses," Nature **409**, 490–493 (2001).
7. K. F. Reim, P. Michelberger, K. C. Lee, J. Nunn, N. K. Langford, and I. A. Walmsley, "Single-photon-level quantum memory at room temperature," Phys. Rev. Lett. **107**, 053603 (2011).
8. A. L. Alexander, J. J. Longdell, M. J. Sellars, and N. B. Manson, "Photon echoes produced by switching electric fields," Phys. Rev. Lett. **96**, 043602 (2006).
9. M. Hosseini, B. M. Sparkes, G. Campbell, P. K. Lam, and B. C. Buchler, "High efficiency coherent optical memory with warm rubidium vapour," Nat. Commun. **2**, 174 (2011).
10. M. P. Hedges, J. J. Longdell, Y. Li, and M. J. Sellars, "Efficient quantum memory for light," Nature **465**, 1052–1056 (2010).
11. H. de Riedmatten, M. Afzelius, M. U. Staudt, C. Simon, and N. Gisin, "A solid-state light-matter interface at the single-photon level," Nature **456**, 773–778 (2008).
12. C. Clausen, I Usmani, F. Bussières, N. Sangouard, M. Afzelius, H. de Riedmatten, and N. Gisin, "Quantum storage of photonic entanglement in a crystal," Nature **469**, 508–512 (2011).
13. E. Saglamyurek, N. Sinclair, J. Jin, J. A. Slater, D. Oblak, F. Bussières, M. George, R. Ricken, W. Sohler, and W. Tittel, "Broadband waveguide quantum memory for entangled photons," Nature **469**, 512–515 (2011).
14. E. Saglamyurek, N. Sinclair, J. Jin, J. A. Slater, D. Oblak, F. Bussières, M. George, R. Ricken, W. Sohler, and W. Tittel, "Conditional detection of pure quantum states of light after storage in a Tm-Doped waveguide," Phys. Rev. Lett. **108**, 083602 (2012).

#172649 - $15.00 USD Received 16 Jul 2012; revised 11 Sep 2012; accepted 28 Sep 2012; published 8 Oct 2012

15. J. Wen and M. H. Rubin, "Theory of two-photon interference in an electromagnetically induced transparency system," Phys. Rev. A **70**, 063806 (2004).
16. T. Chanelière, D. N. Matsukevich, S. D. Jenkins, S. -Y. Lan, T. A. B. Kennedy, and A. Kuzmich, "Storage and retrieval of single photons transmitted between remote quantum memories," Nature **438**, 833–836 (2005).
17. M. D. Eisaman, A. André, F. Massou, M. Fleischhauer, A. S. Zibrov and M. D. Lukin, "Electromagnetically induced transparency with tunable single-photon pulses," Nature **438**, 837–841 (2005).
18. K. S. Choi, H. Deng, J. Laurat, and H. J. Kimble, "Mapping photonic entanglement into and out of a quantum memory," Nature **452**, 67–71 (2008).
19. K. Honda, D. Akamatsu, M. Arikawa, Y. Yokoi, K. Akiba, S. Nagatsuka, T. Tanimura, A. Furusawa, and M. Kozuma, "Storage and retrieval of a squeezed vacuum," Phys. Rev. Lett. **100**, 093601 (2008).
20. J. Appel, E. Figueroa, D. Korystov, M. Lobino, and A. I. Lvovsky, "Quantum memory for squeezed light," Phys. Rev. Lett. **100**, 093602 (2008).
21. H. Zhang, X.-M. Jin, J. Yang, H.-N. Dai, S.-J. Yang, T.-M. Zhao, J. Rui, Y. He, X. Jiang, F. Yang, G.-S. Pan, Z.-S. Yuan, Y. Deng, Z.-B. Chen, X.-H. Bao, S. Chen, B. Zhao, and J.-W. Pan, "Preparation and storage of frequency-uncorrelated entangled photons from cavity-enhanced spontaneous parametric downconversion," Nat. Photonics **5**, 628–632 (2011).
22. B. Zhao, Y.-A. Chen, X.-H. Bao, T. Strassel, C.-S. Chuu, X.-M. Jin, J. Schmiedmayer, Z.-S. Yuan, S. Chen, J.-W. Pan, "A millisecond quantum memory for scalable quantum networks," Nat. Phys. **5**, 95–99 (2009).
23. M. Lettner, M. Mücke, S. Riedl, C. Vo, C. Hahn, S. Baur, J. Bochmann, S. Ritter, S. Dürr, and G. Rempe, "Remote entanglement between a single atom and a Bose-Einstein condensate," Phys. Rev. Lett. **106**, 210503 (2011).
24. M. Varnava, D. E. Browne, and T. Rudolph, "Loss tolerance in one-way quantum computation via counterfactual error correction," Phys. Rev. Lett. **97**, 120501 (2006).
25. S. Zhang, J. F. Chen, C. Liu, S. Zhou, M. M. T. Loy, G. K. L. Wong, and S. Du, "A dark-line two-dimensional magneto-optical trap of ^{85}Rb atoms with high optical depth," Rev. Sci. Instrum. **83**, 073102 (2012).
26. S. Zhang, J. F. Chen, C. Liu, M. M. T. Loy, G. K. L. Wong, and S. Du, "Optical precursor of a single photon," Phys. Rev. Lett. **106**, 243602 (2011).
27. S. Du, P. Kolchin, C. Belthangady, G. Y. Yin, and S. E. Harris, "Subnatural linewidth biphotons with controllable temporal length," Phys. Rev. Lett. **100**, 183603 (2008).
28. P. Kolchin, C. Belthangady, S. Du, G. Y. Yin, and S. E. Harris, "Electro-optic modulation of single photons," Phys. Rev. Lett. **101**, 103601 (2008).
29. P. Grangier, G. Roger, and A. Aspect, "Experimental evidence for a photon anticorrelation effect on a beam splitter: a new light on single-photon interferences," Europhys. Lett. **1**, 173–179 (1986).
30. S. Du, J. Wen, and M. H. Rubin, "Narrowband biphoton generation near atomic resonance," J. Opt. Soc. Am. B **25**, C98–C108 (2008).
31. J. F. Clauser, "Experimental distinction between the quantum and classical field-theoretic predictions for the photoelectric effect," Phys. Rev. D **9**, 853–860 (1974).
32. I. Novikova, A. V. Gorshkov, D. F. Phillips, A. S. Sørensen, M. D. Lukin, and R. L. Walsworth, "Optimal control of light pulse storage and retrieval," Phys. Rev. Lett. **98**, 243602 (2007).
33. S. Zhang, S. Zhou, M. M. T. Loy, G. K. L. Wong, and S. Du, "Optical storage with electromagnetically induced transparency in a dense cold atomic ensemble," Opt. Lett. **36**, 4530-4532 (2011).
34. S. Du, C. Belthangady, P. Kolchin, G. Y. Yin, and S. E. Harris, "Observation of optical precursors at the biphoton level," Opt. Lett. **33**, 2149–2151 (2008).
35. A. V. Gorshkov, A. André, M. Fleischhauer, A. S. Sørensen, and M. D. Lukin, "Universal approach to optimal photon storage in atomic media," Phys. Rev. Lett. **98**, 123601 (2007).
36. S. E. Harris, "Chirp and compress: toward single-cycle biphotons," Phys. Rev. Lett. **98**, 063602 (2007).
37. S. Sensarn, G. Y. Yin, and S. E. Harris, "Generation and compression of chirped biphotons," Phys. Rev. Lett. **104**, 253602 (2010).

1. Introduction

Storage and retrieval of single photons with preserved quantum states is of great importance for long-distance quantum communication and quantum computation [1–3]. A practical quantum memory is desirable with high storage efficiency, long coherence time, and low noise. In the past decade, many schemes have been proposed and demonstrated for optical storage based on coherent light-matter interactions, such as electromagnetically induced transparency (EIT) [4–6], off-resonance Raman interaction [7], and photon echo [8]. Of these techniques, photon echo has recently become attractive due to its promising storage efficiency (as high as 87% [9]), large mode capacity, and compatibility with solid state interfaces [10, 11]. However, these experimental demonstrations of high efficiency were all limited to coherent light pulses, and

#172649 - $15.00 USD Received 16 Jul 2012; revised 11 Sep 2012; accepted 28 Sep 2012; published 8 Oct 2012

the recent implementations with entangled photons [12–14] only achieved a highest memory efficiency of 21% [12].

On the other hand, the EIT memory is compatible with quantum state operations of single-photon wave packets [15–18] and squeezed states [19, 20]. Recent progress includes storing narrow-band single photons generated from atomic systems [16–18] and spontaneous parametric down conversion [21]. Also, the EIT memory time has been pushed to milliseconds by prolonging the ground-state coherence [22]. However, EIT quantum memories have suffered from low efficiency so far, with the highest single-photon storage efficiency being only 17% [18,23], preventing the scheme from practical applications.

In this paper, we report an experimental demonstration of efficient storage and retrieval of narrow-band single-photon waveforms using EIT in a cold atomic ensemble. With the ability to control both single-photon wave packets and the memory bandwidth, we obtain a storage efficiency up to (49±3)% while the nonclassical property is maintained. To our knowledge, it represents the highest storage efficiency for a single-photon waveform to date. Because an efficiency above 50% is necessary to operate a memory for error correction protocols in one-way quantum computation [24], our result brings the atomic quantum light-matter interface closer to practical quantum information applications [10].

2. Experimental setup

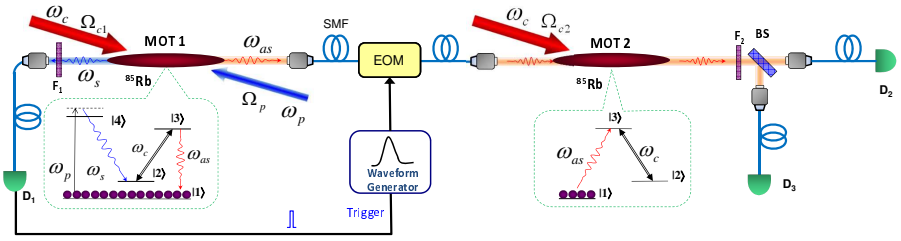

Fig. 1. Schematics of the experimental setup for storage and retrieval of heralded single photons with controllable waveforms. The ^{85}Rb energy levels are chosen as $|1\rangle = |5S_{1/2}, F = 2\rangle$, $|2\rangle = |5S_{1/2}, F = 3\rangle$, $|3\rangle = |5P_{1/2}, F = 3\rangle$ and $|4\rangle = |5P_{3/2}, F = 3\rangle$. In MOT1, with the presence of pump (ω_p) and coupling (ω_c) lasers, we produce counter-propagating Stokes (ω_s) and anti-Stokes (ω_{as}) photon pairs. Conditioned on detection of the Stokes photon, its paired anti-Stokes photon passes through an electro-optical modulator (EOM) and is stored in MOT2. F_1 and F_2 are two narrow-band optical filters.

Figure 1 illustrates the experimental configuration we use to generate, store, and retrieve narrow-band single photons. We make use of two two-dimensional (2D) ^{85}Rb magneto-optical traps (MOT1 and MOT2) with high optical depth (OD), which are described in details in [25]. The similar setup has been also used for producing and observing single-photon optical precursors [26]. Each cold atomic cloud, with a temperature of about 100 μK, has a length of 1.7 cm and transverse diameter of 0.7 mm. From MOT1, we produce Stokes (ω_s) and anti-Stokes (ω_{as}) paired photons [27], with the presence of counter-propagating pump (ω_p, 780nm) and coupling (ω_c, 795nm) beams aligned at a 3° angle with respect to the Stokes-anti-Stokes axis. The pump laser is blue detuned by 60 MHz from the $|1\rangle \rightarrow |4\rangle$ transition. The coupling laser is on resonance with the $|2\rangle \rightarrow |3\rangle$ transition. Both the pump and coupling lasers have the same collimated beam diameter of 1.6 mm and their linewidths are narrower than 1 MHz. The Stokes and anti-Stokes photons are coupled into two opposing single-mode fibers (SMF). When the Stokes photon is detected by the single-photon detector D_1, we send its paired anti-Stokes photon through an amplitude electro-optical modulator (EOM, 10 GHz, EOspace), which is driven

#172649 - $15.00 USD Received 16 Jul 2012; revised 11 Sep 2012; accepted 28 Sep 2012; published 8 Oct 2012

by a triggered waveform generator. In this way, we are able to generate heralded single anti-Stokes photons with controllable waveforms [28]. We then store the anti-Stokes photons in the cold atoms at MOT2, controlled by a second coupling beam directed from the same coupling laser in MOT1. The anti-Stokes photon single mode is focused to the center of MOT2 along its longitudinal axis and has a $1/e^2$ diameter of 245 μm at the waist. The coupling beam at MOT2, with a $1/e^2$ diameter of 1.0 mm, is aligned at a 3° angle with respect to the anti-Stokes propagation. We run the experiment periodically with a MOT time of 4.5 ms followed by a photon generation window of 0.5 ms for each cycle. The MOT magnetic fields remain on all the time. In both MOTs, at end of the trapping time, we optically pump all the atoms to the ground level $|1\rangle$. Coincidence counts are recorded by a time-to-digital converter (Fast Comtec P7888) with 1 ns bin width.

3. Single-photon storage

The physical mechanism of EIT memory has been well studied in terms of dark-state polaritons [5]. As the photon wave packet is spatially compressed inside the medium, we turn off the coupling laser to adiabatically convert the photon state into a long-lived atomic spin wave that involves only the two ground levels $|1\rangle$ and $|2\rangle$. After a controllable time delay, we turn on the coupling laser again to retrieve the photon wave packet. There are two important parameters characterizing the performance of a single-photon memory. The first is the storage efficiency, defined as the probability of storing and retrieving the single photon,

$$\eta = \frac{\int |\psi_{out}(\tau)|^2 d\tau}{\int |\psi_{in}(\tau)|^2 d\tau}, \tag{1}$$

where $\psi_{in}(\tau)$ and $\psi_{out}(\tau)$ are the input and output heralded single-photon wave packets with $\tau = t_{as} - t_s$. The storage efficiency is determined by both the photon temporal waveform and the EIT memory bandwidth. The second parameter is the storage time, which is limited by the ground-state coherence time. In this work, we focus on the storage efficiency at two pulse-length storage time. Moreover, a single photon storage requires the memory to be operated at an ultra-low noise level. For the EIT memory, the major noise comes from the scattering of the coupling laser beam. Compared to warm atomic vapor cells that require a collinear Doppler-free optical setup [17], this scattering is suppressed in our cold atom system because of the 3° angle between the coupling beam and the anti-Stokes photons. Further noise reduction is accomplished by two optical frequency filters (F_1 and F_2, with a bandwidth of 0.5 GHz). A beam splitter (BS) and two detectors (D_2 and D_3) are used to verify the single-photon quantum nature, because a single photon incident at a BS must go to one port or the other. A measure of the quality of heralded single photons is given by the conditional correlation function [29]

$$g_c^{(2)} = \frac{N_{123} N_1}{N_{12} N_{13}}, \tag{2}$$

where N_1 is the Stokes counts at D_1, N_{12} and N_{13} are the twofold coincidence counts, and N_{123} is the threefold coincidence counts. A classical field must satisfy $g_c^{(2)} \geq 1$. A pure single photon has $g_c^{(2)} = 0$ and a two-photon state has $g_c^{(2)} = 0.5$. Therefore $g_c^{(2)} < 1.0$ violates the classical limit and $g_c^{(2)} < 0.5$ suggests the near-single-photon character.

We first characterize the photon source. In the following experiments, we fix the pump and coupling laser Rabi frequencies during the biphoton generation in MOT1 at $\Omega_p = 0.4\gamma_{13}$ and $\Omega_{c1} = 5.1\gamma_{13}$, where $\gamma_{13} = 2\pi \times 3$ MHz is the electric dipole relaxation rate between $|1\rangle$ and $|3\rangle$. The optical depth of MOT2 is maintained at OD_2=60. By varying the OD at MOT1 (OD_1), we produce paired photons with controllable temporal length [27]. At a low OD_1, the two-photon temporal correlation time length is determined by $1/(\gamma_{13} + \gamma_{12}) \simeq 1/\gamma_{13} = 53$ ns, where

#172649 - $15.00 USD Received 16 Jul 2012; revised 11 Sep 2012; accepted 28 Sep 2012; published 8 Oct 2012

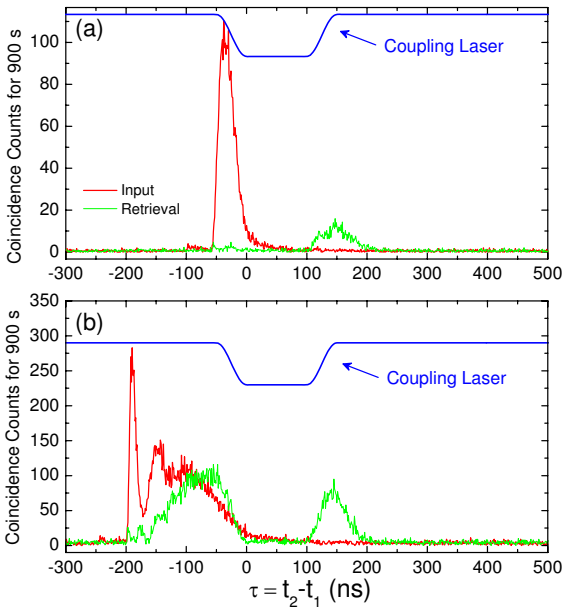

Fig. 2. Direct storage and retrieval of single photons without waveform shaping. Single photons with (a) a short waveform and (b) a long waveform are produced from MOT1 at OD_1=7 and 35, respectively. The coincidence counts are recorded by D_1 and D_2. Other parameters are OD_2=60, $\Omega_{c2} = 11\gamma_{13}$, and $\gamma_{12} = 0.03\gamma_{13}$.

$\gamma_{12} \simeq 0.03\gamma_{13}$ is the ground-state dephasing rate [30]. At a high OD_1, we enter the group delay regime where the photon pair temporal length is determined by the relative group delay time between the paired anti-Stokes and Stokes photons [30]. The red curves in Fig. 2 show the two-photon coincidence counts between detectors D_1 and D_2 with 1 ns bin width, collected for 900 s. At OD_1=7, the heralded anti-Stokes photon has a temporal length of about 50 ns, as shown in Fig. 2(a), while at OD_1=35 we prolong the length to 200 ns as shown in Fig. 2(b). Excluding the uncorrelated accidental coincidences, there are a total of 3300 (or 18100) biphoton coincidence counts detected by D_1 and D_2 for OD_1=7 (or 35), which is consistent with the theoretical prediction at the group delay regime where the total rate of paired counts scales linearly as OD_1 [30]. This is because the on-resonance spectral brightness is proportional to OD_1^2 but the bandwidth reduces linearly with OD_1. Including the coincidence counts between D_1 and D_3 (the measured BS splitting ratio is about 45%:55%), we detect a total of 7400 (or 42400) photon pairs in 900 s, corresponding to a photon pair detection rate of 8 (or 47) pair/s. Taking into account the detector quantum efficiencies (50% each), fiber-fiber coupling efficiencies (70% at MOT1 and 72% at MOT2), EOM transmission (50%), fiber connection efficiency (61%), filter transmissions (65% each), and the duty cycle (10%), this corresponds to a generation rate of about 4900 (or 28900) pair/s from MOT1. At OD_1=7 (or 35), for each click at D_1, the success probability of detecting its heralded photon at D_2 and D_3 is 2.8% (or 4.1%), which, accounting all the losses and efficiencies, corresponds to a pairing efficiency of 56% (or 82%) when they are produced from MOT1. The incident anti-Stokes photon rate in MOT2 is about 1000/s (or 6200/s). The nonclassical properties of the paired photons can be measured by violation of the Cauchy-Schwartz inequality $[g^{(2)}_{i,j}(\tau)]^2/[g^{(2)}_{i,i}(0)g^{(2)}_{j,j}(0)] \leq 1$ [31]. Because the paired photons are generated through spontaneous four-wave mixing, there is no correlation between different pairs. Therefore, the correlation function $g^{(2)}_{s,as}(\tau)$ can be obtained by nor-

#172649 - $15.00 USD Received 16 Jul 2012; revised 11 Sep 2012; accepted 28 Sep 2012; published 8 Oct 2012

malizing the two-photon coincidence counts to the background floor resulting from accidental coincidences between uncorrelated photons. We obtain $g^{(2)}_{s,as}(\tau)$ with maximum values of 150 and 95 for the input waveforms in Fig. 2(a) and (b), respectively. With $g^{(2)}_{s,s}(0) = g^{(2)}_{as,as}(0) = 2.0$ measured using a fiber beam splitter, we obtain a violation of the inequality by a factor of 5625 and 2256, respectively. To characterize the single-photon nature of the heralded photons, we measure $g^{(2)}_c = 0.10 \pm 0.02$ for the short photon (with a coincidence window of 100 ns) and $g^{(2)}_c = 0.17 \pm 0.02$ for the long photon (with a coincidence window of 200 ns), each with a total time of 2100 s.

We then measure the storage efficiency without shaping the waveform of anti-Stokes photons by leaving the EOM at its maximum transmission. To store the anti-Stokes photon, we switch off the coupling laser at MOT2 ($\Omega_{c2} = 11\gamma_{13}$) for a period of 100 ns after detecting its paired Stokes photon. The retrieved photon waveforms are displayed as the green curves in Fig. 2(a) and (b). The coupling laser has switch-on and -off times of 50 ns. For both waveforms, we obtain the same storage efficiency of (20±2)%. The measured $g^{(2)}_c = 0.24 \pm 0.17$ and 0.44 ± 0.15 confirm that we indeed retrieve single photons. However, in both cases, the waveform profiles are not preserved after retrieval.

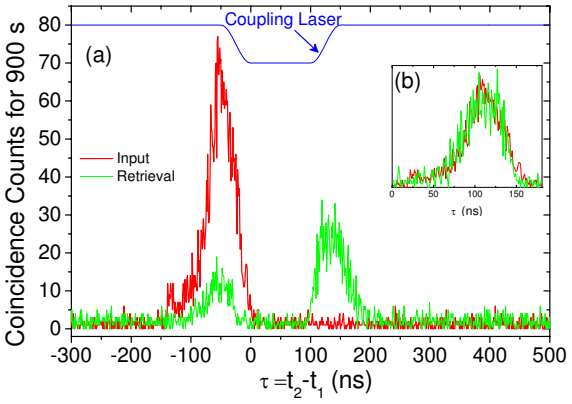

Fig. 3. Storage and retrieval of a single photon with optimal waveform. (a) The optimal input (red curve) and output (retrieval, green curve) heralded single-photon waveforms are measured as coincidence counts between D_1 and D_2. (b) The inset shows the time-reversed retrieved photon waveform matches the input photon waveform after normalization. The operating parameters at MOT2 are OD_2=60, $\Omega_{c2} = 11\gamma_{13}$, and $\gamma_{12} = 0.03\gamma_{13}$. The measured storage efficiency is (36±3)%.

Previous work for coherent pulse storage suggests that the storage efficiency can be substantially improved by optimizing the pulse shape to match the EIT bandwidth. We follow the optimization procedure described in [32, 33]. We work with the initial waveform in Fig. 2(b). The oscillatory structure on top of the leading edge is an optical precursor at the single-photon level [26, 27, 34], which is produced from the optical frequency components far away from the atomic resonance and whose wave front always travels at the speed of light in vacuum. This optical precursor component cannot be slowed and stored because its frequency components do not fall inside the EIT slow light window [26], thus we remove it from the single-photon waveform by switching on the EOM 100 ns after the leading edge. At MOT2, we fix the coupling laser Rabi frequency as $\Omega_{c2} = 11\gamma_{13}$ and OD_2=60. We feed back the time-reversed waveform of the retrieved photon to shape its input waveform using the EOM. The optimal input-output waveforms for the maximum storage efficiency are obtained after three iterations, as shown

#172649 - $15.00 USD Received 16 Jul 2012; revised 11 Sep 2012; accepted 28 Sep 2012; published 8 Oct 2012

in Fig. 3(a), which becomes identical for more than three iterations and the storage efficiency saturates [32]. The input single-photon waveform has a full width at half maximum (FWHM) of 50 ns and a peak $g^{(2)}_{s,as}$ value of 23. The output single-photon waveform is retrieved after a storage time of 2 pulse length (100 ns). The optimal storage efficiency is (36±3)%. To confirm that at this optimal condition, the retrieved photon waveform is the time-reversal of the input, we plot the time-reversed retrieved photon waveform together with the input waveform with a proper rescaling in the inset [Fig. 3(b)], and they match each other very well. This time-reversal relationship between the input and output waveforms agrees with the theoretical prediction and indicates that the phase coherence information of the single-photon wave packet is preserved during storage [35]. For a quantitative estimation, we calculate the temporal waveform likeness $L = |\int \psi_{in}(\tau)\psi_{out}(-\tau)d\tau|^2/[\int|\psi_{in}(\tau)|^2 d\tau \int|\psi_{out}(\tau)|^2 d\tau]$. Since we work at the group delay regime, the single-photon waveform from MOT1 is nearly transform-limited [26, 30]. After the amplitude modulation by the EOM, we obtain the optimal waveform envelope without time-varying phase. Therefore, we have $\psi_{in}(\tau) = \sqrt{G^{(2)}_{in}(\tau)}$ and $\psi_{out}(\tau) = \sqrt{G^{(2)}_{out}(\tau)}$, where $G^{(2)}_{in}(\tau) = \langle \hat{a}^\dagger_s(t)\hat{a}^\dagger_{as}(t+\tau)\hat{a}_{as}(t+\tau)\hat{a}_s(t)\rangle_{in}$ and $G^{(2)}_{out}(\tau) = \langle \hat{a}^\dagger_s(t)\hat{a}^\dagger_{as}(t+\tau)\hat{a}_{as}(t+\tau)\hat{a}_s(t)\rangle_{out}$ are Glauber correlation functions before and after storage that can be obtained from the coincidence counts in Fig. 3. Here $\hat{a}^\dagger$ and $\hat{a}$ are photon creation and annihilation operators. For this optimal storage, we obtain L=93%. We measure $g^{(2)}_c = 0.30 \pm 0.06$ for the input photon and $g^{(2)}_c = 0.26 \pm 0.13$ for the retrieved photon with a coincidence window of 100 ns and a total time of 3300 s. They are below the two-photon threshold of 0.5.

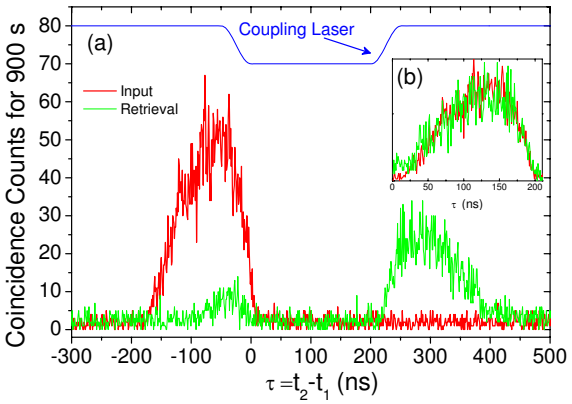

Fig. 4. Optimal storage and retrieval of single photons with reduced ground-state dephasing rate. (a) The optimal input (red curve) and output (retrieval, green curve) heralded single-photon waveforms. (b) The inset shows the time-reversed retrieved photon waveform matches the input photon waveform after normalization. The operating parameters at MOT2 are OD_2=60, $\Omega_{c2} = 6.88\gamma_{13}$, and $\gamma_{12} = 0.01\gamma_{13}$. The measured storage efficiency is (49±3)%.

The storage efficiency is also affected by the dephasing rate γ_{12} between the two ground levels $|1\rangle$ and $|2\rangle$ which causes decoherence loss and absorption at high OD. We obtain the effective dephasing rate by best-fitting it to the EIT transmission spectrum. The finite dephasing rate is caused by stray magnetic fields, atomic motion, and the coupling beam profile. In the above measurements, the coupling beam at MOT2 has a diameter of 1.0 mm, and we obtain $\gamma_{12} = 0.03\gamma_{13}$. To reduce the dephasing rate, we increase the coupling beam diameter to 1.6 mm and obtain $\gamma_{12} = 0.01\gamma_{13}$. The coupling laser power, which is limited by the maximum power allowed by the fiber EOM, remains the same as that in the previous measurements and

#172649 - $15.00 USD Received 16 Jul 2012; revised 11 Sep 2012; accepted 28 Sep 2012; published 8 Oct 2012

thus we have $\Omega_{c2} = 6.88\gamma_{13}$. Figure 4(a) shows the optimal storage and retrieval of single photon waveforms under the new conditions. Due to the narrower EIT bandwidth, the optimal waveform has a longer temporal length (FWHM=100 ns) and a peak $g^{(2)}_{s,as}$ value of 12. For a delay of two pulse length (200 ns), we obtain a storage efficiency of (49±3)%. The inset shows that the suitably rescaled time-reversed output waveform matches the input waveform well [Fig. 4(b)]. We obtain a temporal waveform likeness of L=96%. For the conditional correlation measurement, we take the FWHM (100 ns) as the coincidence window and obtain $g^{(2)}_c = 0.10 \pm 0.06$ for the input waveform and $g^{(2)}_c = 0.14 \pm 0.14$ for the retrieved photon. The higher $g^{(2)}_c$ after retrieval is caused by the single photon storage loss in presence of detector dark counts and multiphoton events from the background noise photons. As we increase the coincidence window to 200 ns to contain more accidental counts from noise photons and dark counts, the $g^{(2)}_c$ of the input and retrieved photon become 0.28 ± 0.07 and 0.66 ± 0.22 respectively, which are still below the classical limit. The measured memory lifetime is about 1.6 μs, which is mainly determined by the inhomogeneous MOT magnetic field.

In our configuration, we find that the connection between $g^{(2)}_c$ and the normalized cross correlation function $\bar{g}^{(2)}_{s,as}$ (averaged over the same coincidence window) can be expressed as $g^{(2)}_c \simeq (2\bar{g}^{(2)}_{s,as} + 1)/[(\bar{g}^{(2)}_{s,as} + 1)^2]$. In the case $\bar{g}^{(2)}_{s,as} >> 1$, this reduces to $g^{(2)}_c \simeq 2/\bar{g}^{(2)}_{s,as}$, which agrees with our experimentally measured values within their statistical errors. As we increase the coincidence window length, $g^{(2)}_c$ increases because of an increasing probability of detecting multiphoton events from uncorrelated noise photons and dark counts. Oppositely, $\bar{g}^{(2)}_{s,as}$ drops as the coincidence window length increases. As a measure of the ratio of correlated photons (signal) to uncorrelated photons (noise), $\bar{g}^{(2)}_{s,as}$ provides a quick estimate of the quality of heralded single photons. It is clear that both $g^{(2)}_c < 1$ and the violation of Cauchy-Schwartz inequality require $\bar{g}^{(2)}_{s,as} > 2$ for beating the classical limit. $\bar{g}^{(2)}_{s,as} > 4$ indicates the near-single-photon character of the heralded anti-Stokes photon ($g^{(2)}_c < 0.5$).

4. Conclusion

In summary, we have demonstrated optimal storage and retrieval of heralded single-photon wave packets using EIT in cold atoms. At a high OD of 60, we obtain a storage efficiency of close to 50% for the optimal single-photon waveform with a temporal likeness of 96%. In our experiment, the storage efficiency might be limited by the inhomogeneous stray magnetic field, the coupling beam profile, atomic motion, and possibly some nonlinear processes at high optical depth. The storage efficiency in this work refer only to the capability of the EIT atomic medium at MOT2 in storing and retrieving optimal single-photon waveforms, and it does not include the fiber connection loss and the EOM insertion loss. The EOM amplitude modulation loss of about 50% in our system can be counted into the heralded single-photon generation efficiency. This modulation loss can be eliminated, in principle, using other waveform shaping techniques, such as chirp (using phase-frequency modulation) and compression [36, 37].

Acknowledgments

The work was supported by the Hong Kong Research Grants Council (Project No. 601411). J. W. was supported by an AI-TF New Faculty Grant and an NSERC Discovery Grant.